NEPSC2: The SCUBA-2 850μm survey in the North Ecliptic Pole

JCMT Users Meeting 2022
2022.02.25.

Hyunjin Shim (KNU, Korea) on behalf of the NEP team

Cosmic history - star formation and galaxy evolution

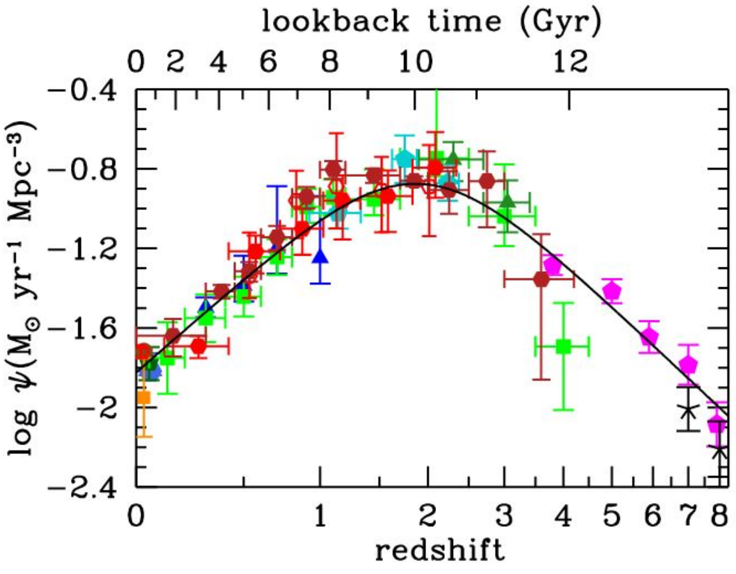

cosmic star formation history, Madau & Dickinson (2014)

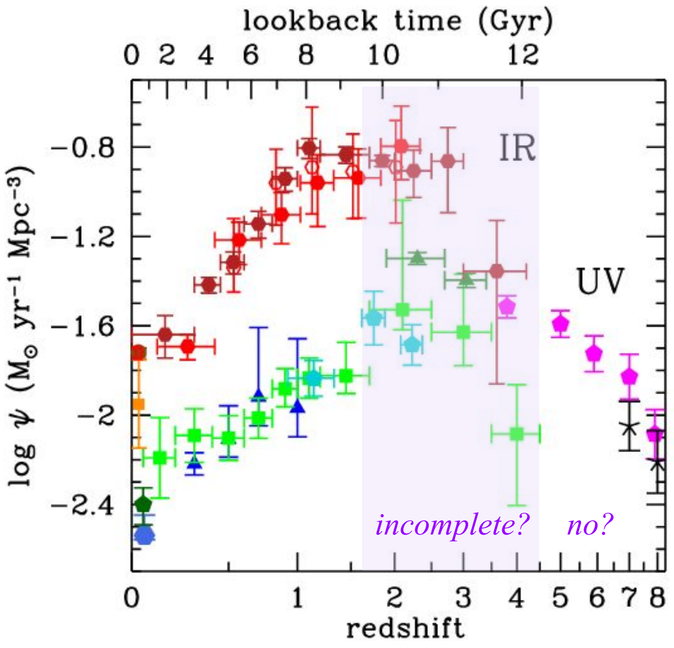

(when UV-SFR is uncorrected for dust attenuation)

Our understanding on the “dusty” star formation is still limited, which requires large FIR/(sub)mm surveys

Selection of dusty galaxies with large star formation - submillimetre

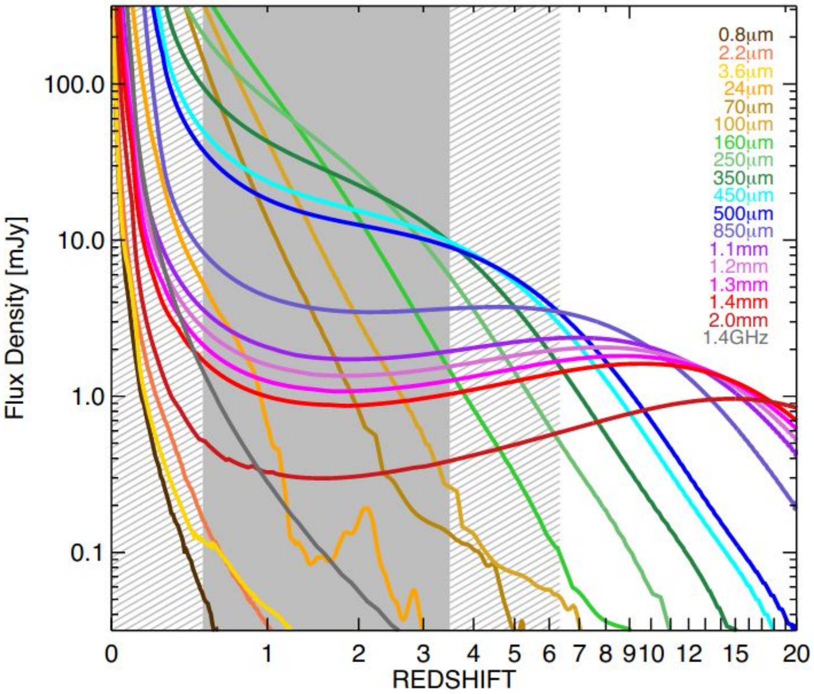

observed flux densities for $10^{12.5}$ L_{solar} galaxy at different redshift (Casey et al. 2014)

dusty star-forming galaxies

(more general term; see review by Casey et al. 2014)

- large stellar mass ($10^{10\text{-}11}$ M_{solar})
- large SFR (100-1000 M_{solar} yr^{-1})
- gas rich (selected samples, up to z>4)
- frequently associated w/ AGN

Therefore SMGs are suspected to be ancestors of the most massive galaxies, and reproducing the observed properties of the SMGs through the galaxy formation model is still underway.

- number counts, redshift distribution

(extragalactic) Far-Infrared/Submillimeter surveys

There exist so many "deep fields", with uniqueness/specialty on
low cirrus, deepest, widest, has high spatial resolution optical/NIR images, can be reached by ALMA, …

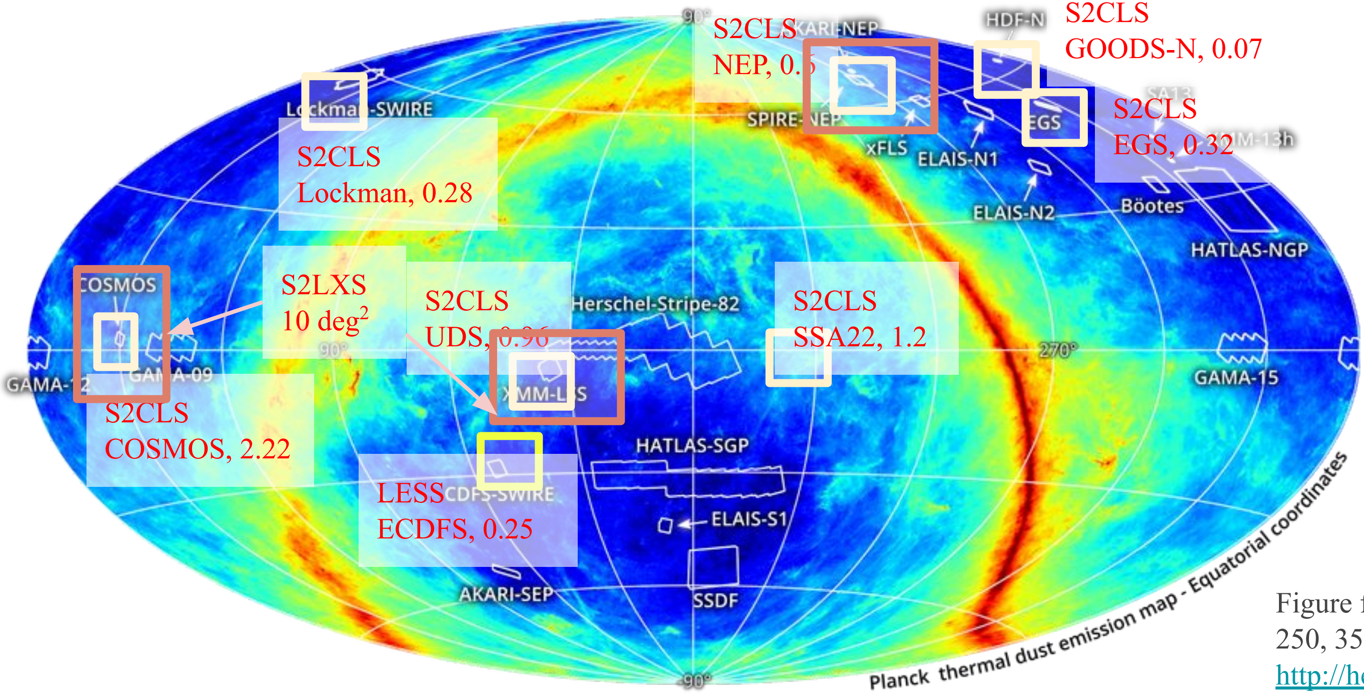

JCMT (15-m)/SCUBA-2
(prev. SCUBA) 450, 850μm
S2CLS, Geach et al. 2017
Large Program ext.(2020A~)

ASTE (10-m)/AzTEC 1.1mm
APEX (12-m)/LABOCA 870μm

LMT (50-m)/TolTEC 1.1, 1.4, 2mm - planned

Figure from Herschel Legacy Project (HELP);
250, 350, 500μm, Shirley et al. 2021
http://hedam.lam.fr/HELP/

Ecliptic Poles

:

High visibility for space-based telescopes on the sun-synchronous polar orbit (AKARI, eROSITA, EUCLID, SPHEREx, …)

multi-wavelength coverage from the previous studies

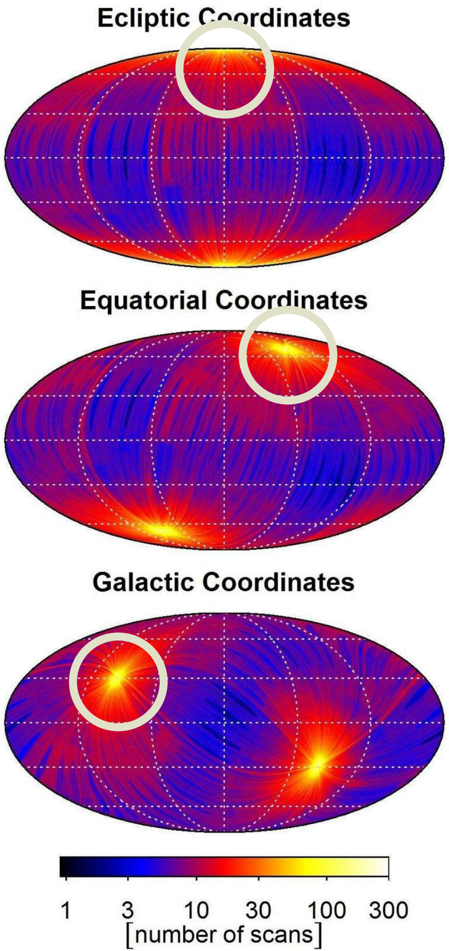

Doi et al.(2015) AKARI FIR all-sky maps

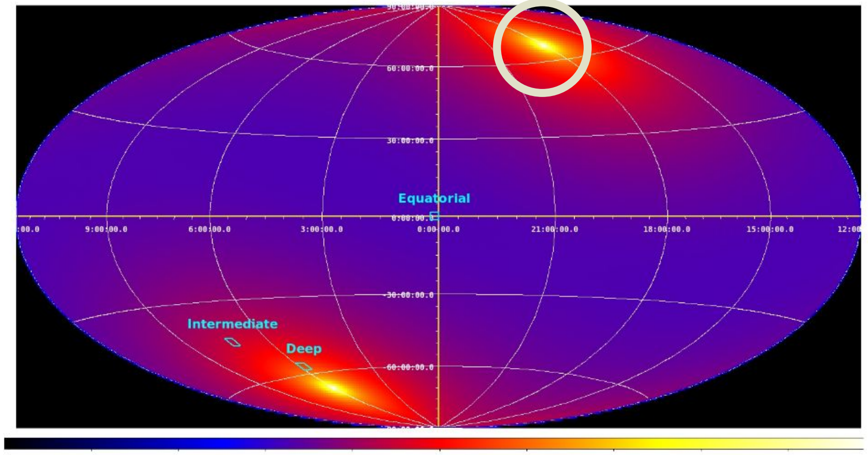

Clerc et al.(2018) eROSITA simulations

THE EUCLID WIDE AND DEEP SURVEYS

imaging + spectroscopy 0.9-2μm

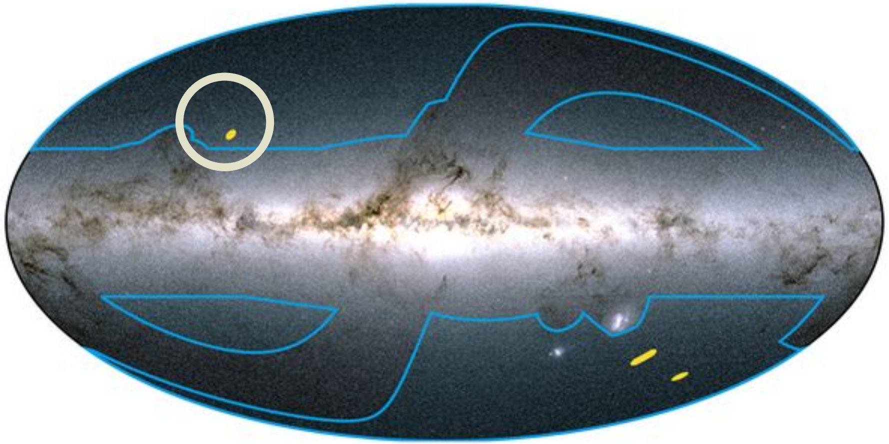

850μm survey on the NEP field (JCMT LP; M17BL007, M20AL005)

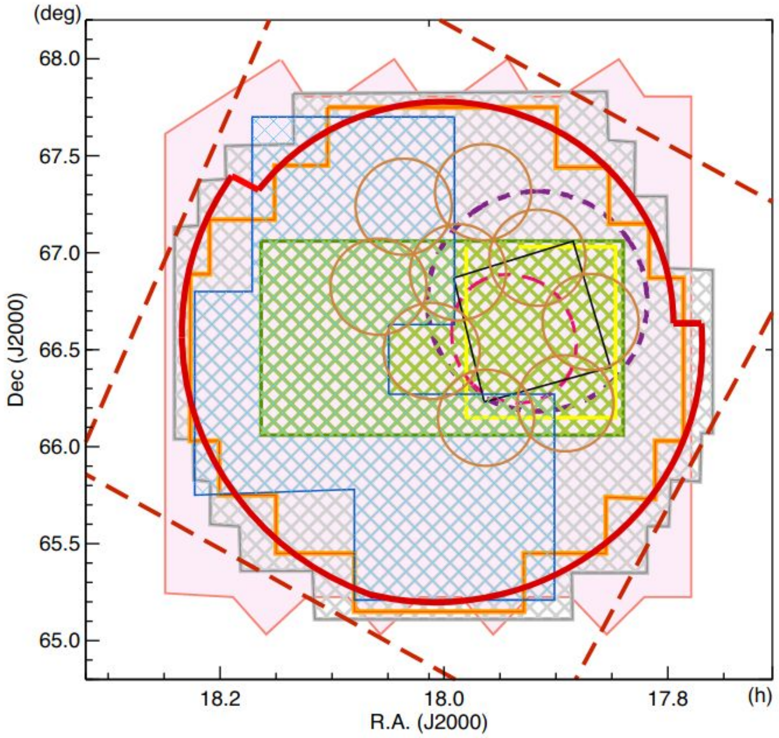

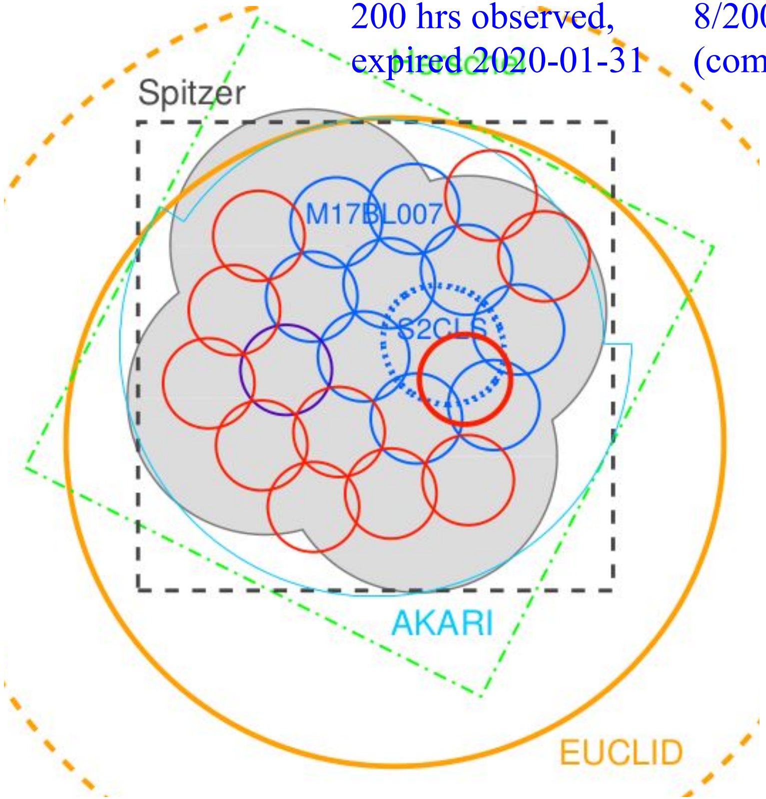

200 hrs observed, expired 2020-01-31

8/200 hrs observed (completion rate **3%**)

Kim et al.(2021) surveys around the NEP

850μm survey on the NEP field (2deg^2) - data obtained before 2020

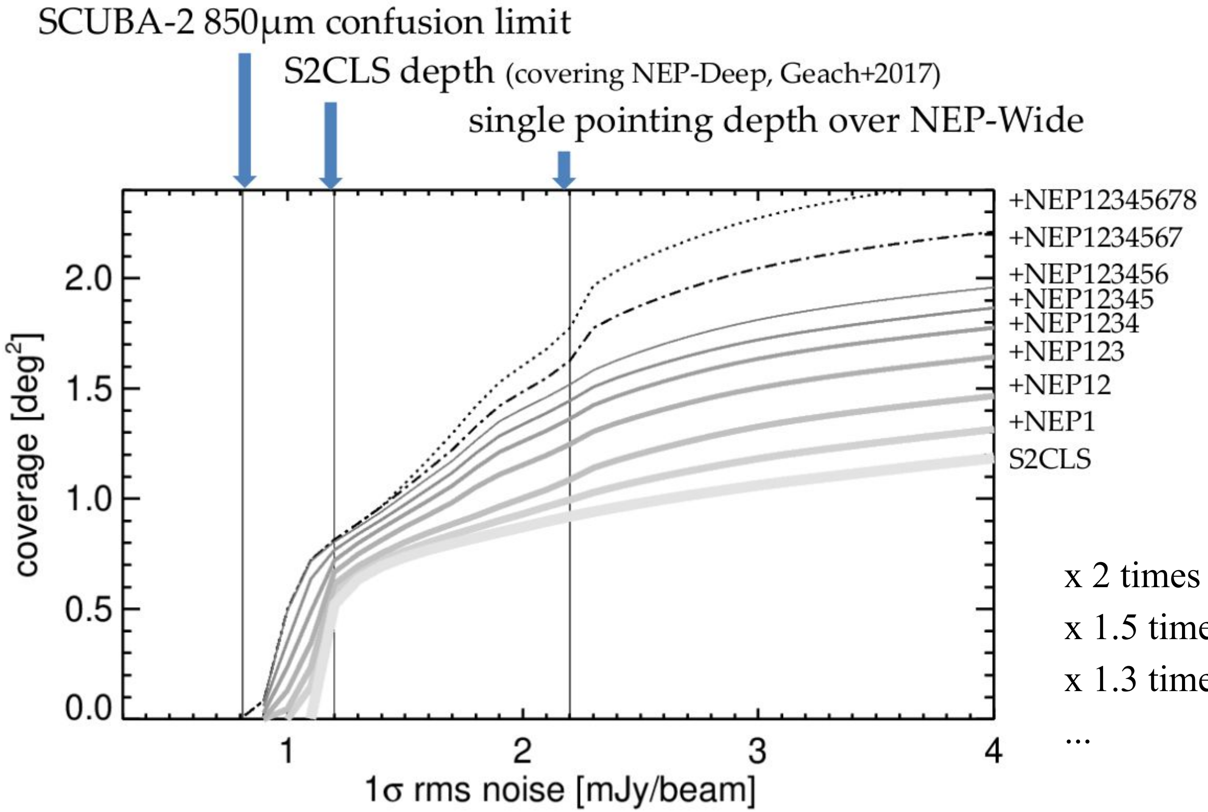

x 2 times wider 2.2 mJy rms

x 1.5 times wider 1.2 mJy rms

x 1.3 times deeper in the deepest region

...

850μm survey on the NEP field (2deg^2) - data obtained before 2020

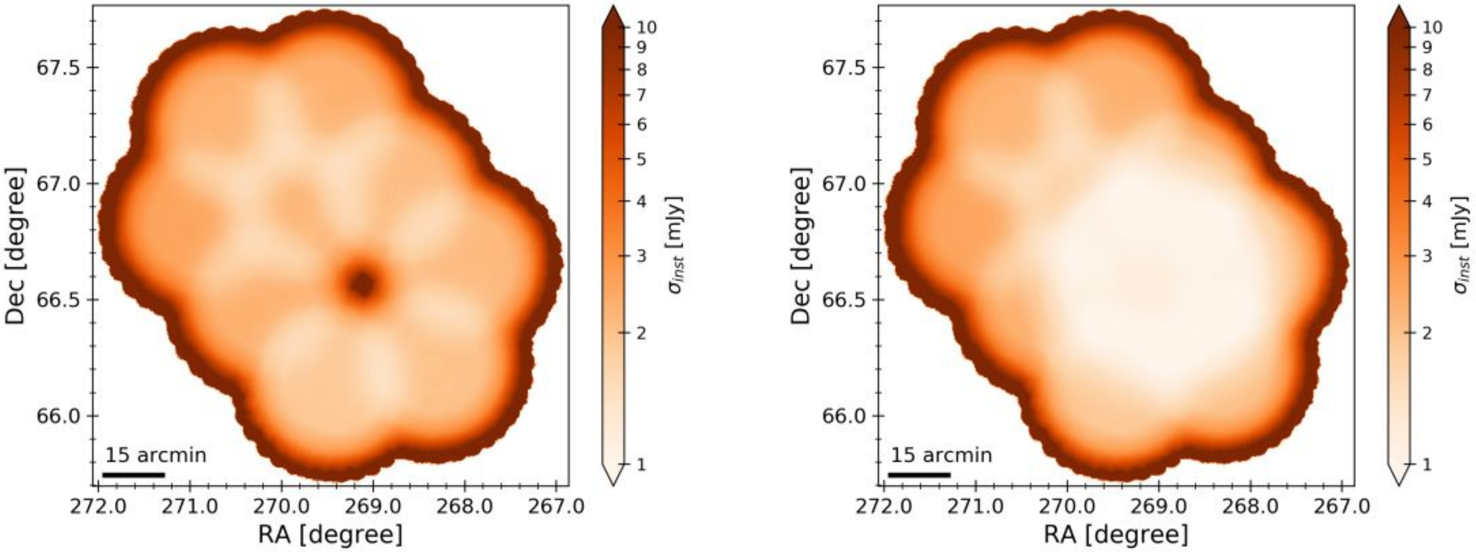

Figure 1. (Left) The noise map over the NEP field through JCMT Large Program M17BL007, based on the data obtained between 2017 and 2019 (9 fields completed). The vacant region in the center is where the previous SCUBA-2 survey (S2CLS; Geach et al. 2017) has covered, which is centered on the pole. In the center of each target field, the sensitivity ranges $\sigma_{\rm inst} = 1.7 - 2$ mJy. With a caution, we consider that fields with < 2.5 mJy rms In its deepest area where more than two target fields overlaps, the map goes as deep as $\sigma_{\rm inst} = 1.4$ mJy.

850μm survey on the NEP field (2deg^2) - data obtained before 2020

data reduction, map creation (using newly obtained data + archival S2CLS data), source extraction, flux deboosting, estimation of false detection rate and completeness

NEPSC2 (Shim+2020)

549 sources (4σ selection, 10% false detection)

342 sources (4.5σ selection, <3% false detection)

647 unique sources

S2CLS (Geach+2017) - NEP

330 sources (3.5σ selection, 20% false detection)

196 sources (4σ selection, 6% false detection)

71 sources (5σ selection, negligible)

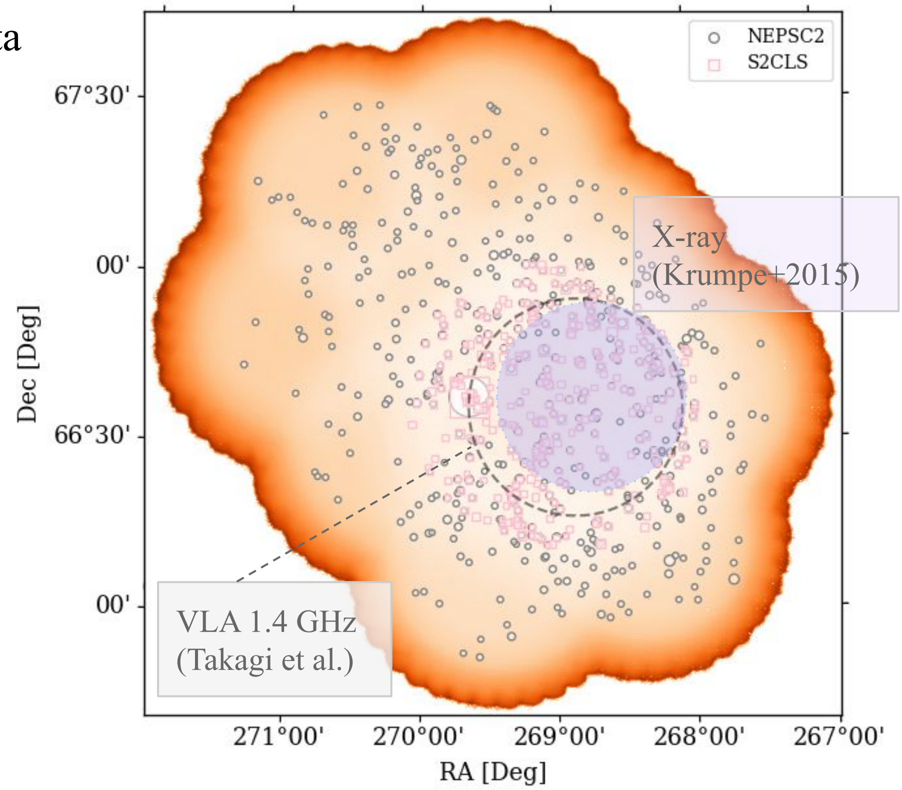

850μm survey on the NEP field (2deg^2)

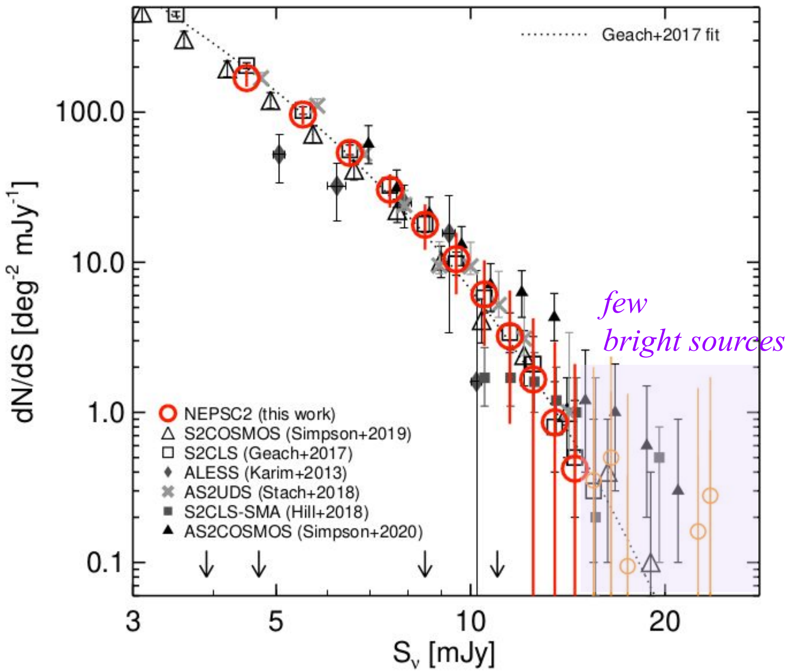

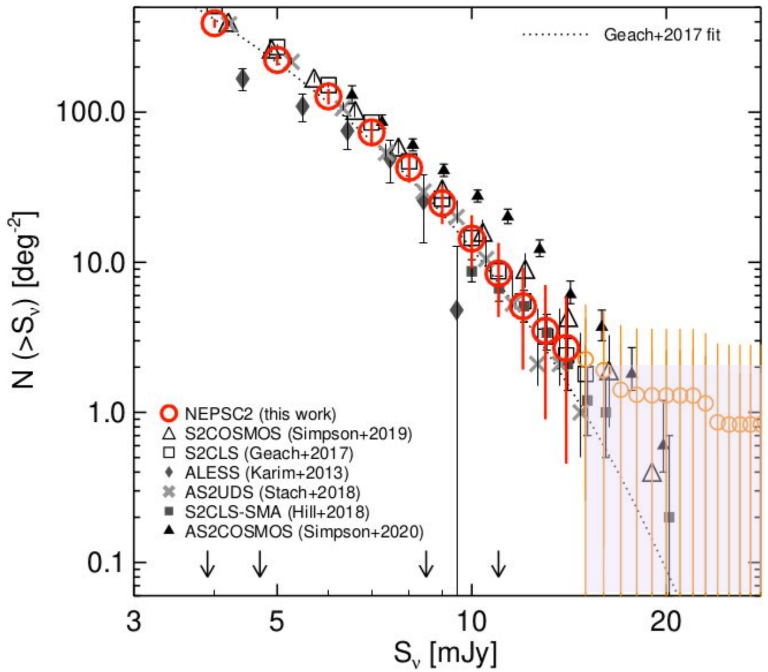

Source number counts are consistent with previous single-dish surveys (S2COSMOS, S2CLS) at 4-15 mJy

Counterpart identification of 850μm sources

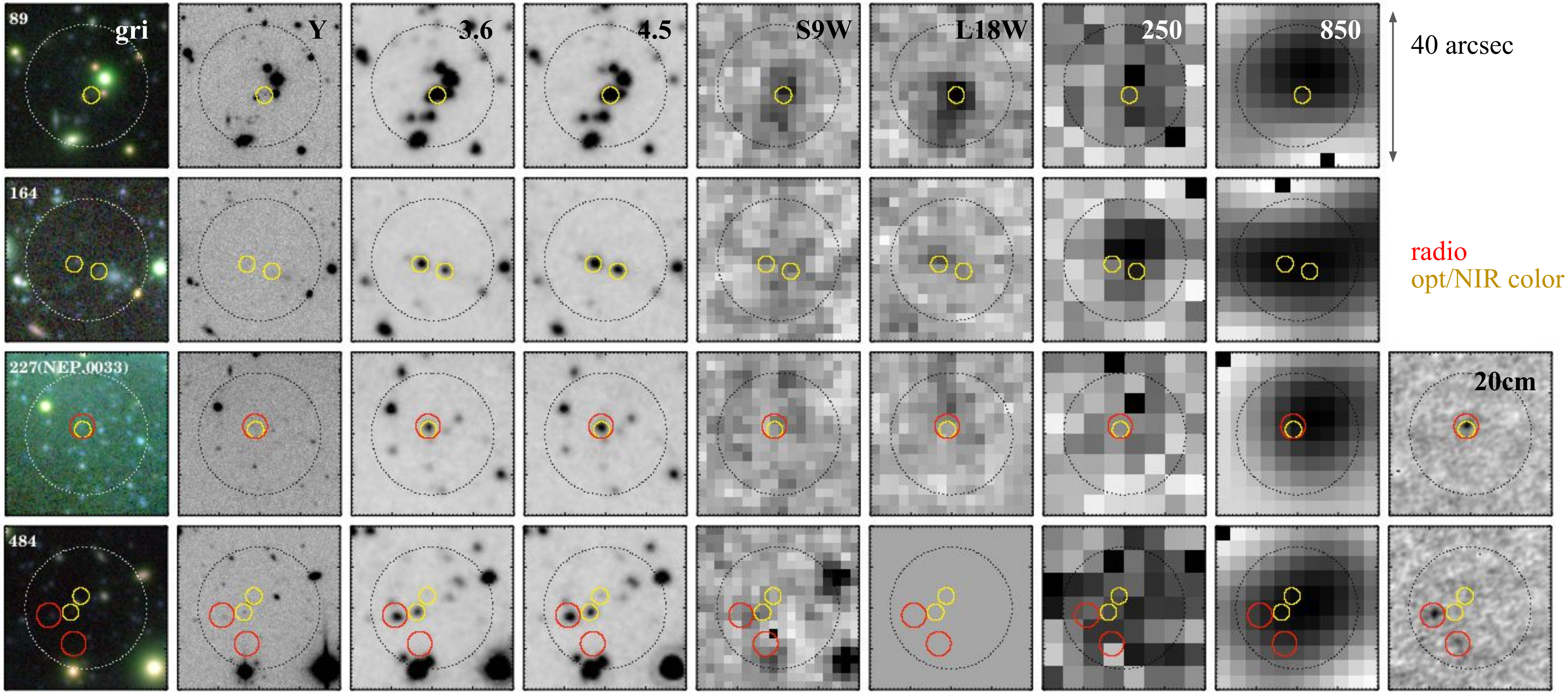

Counterpart identification of 850μm sources

FIR/radio correlation for star-forming galaxies implies that using radio data to find 850μm source counterpart is an efficient way to find counterparts. However, the (radial) areal coverage is limited in our case.

Therefore we calculated probability of "being a true counterpart" and "not being a coincident match" for individual objects within a specific radius around each source, and decided the probable counterparts.

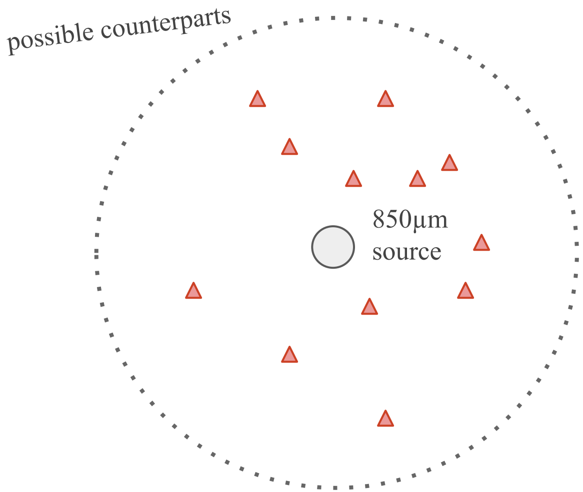

$$LR = \underbrace{\frac{q(m)}{n(m)}}_{\text{mag, color, ...}} \times \underbrace{f(r)}_{\text{positional offset}}$$

$$\begin{aligned} P(D|H) &= P(D_\phi|H) \times P(D_m|H) \\ &= P(D_\phi|H) \times \frac{\bar{q}(m)}{\bar{n}(m)}, \end{aligned}$$

$$p_{\rm any} = 1 - P(H_0|D) / \sum_i P(H_i|D)$$

$$p_i = P(H_i|D) / \sum_{i>0} P(H_i|D)$$

Counterpart identification of 850μm sources

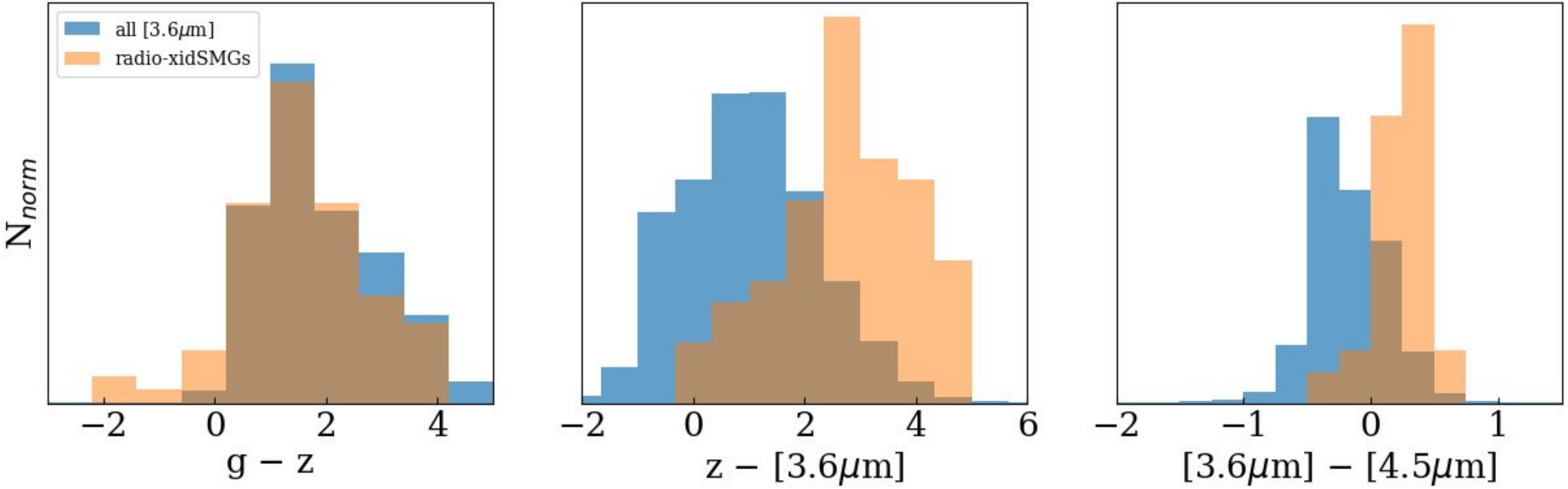

Color distribution of all [3.6μm]-selected objects (i.e., background objects) and radio-identified SMGs. Histograms are 'normalized' to yield the enclosed area to be 1. The SMG population is more clearly distinguished in (z - [3.6μm]) colors and/or ([3.6μm] - [4.5μm]) colors compared to the optical colors, therefore such color distribution could be used to select counterparts in short wavelengths in combination with the spatial offset.

Multi-wavelength photometry for the identified counterparts

Among 647 submillimetre sources,
reliable counterparts are identified for 449 sources
(69 per cent).

Number of identified counterparts is 516.

HSC grizy (Oi+2020; used forcedCat)
IRAC 3.6, 4.5μm
u-band (Takagi/Hwang+2007/Huang+2020)
CFHT ugriz + YJK (Takagi+2012/Oi+2014)
CFHT ugriz (Hwang+2007)
AKARI IRC -deep (Takagi+2012)
AKARI IRC -wide (Kim+2012)
WISE
MIPS 24μm
Herschel PACS
Herschel SPIRE

SED fitting using CIGALE

(to derive redshifts, stellar mass, SFR, AGN fraction, etc.)

CIGALE (Boquien et al. 2019) were run w/ "redshift" mode, *since there are very few objects with spectroscopic redshifts; photometric redshifts are available for only a fraction of objects by different authors*

Model and input parameters	Range
Star-formation history: `sfh2exp`	
e-folding time of the main stellar population model [Myr]	1000, 3000, 5000
e-folding time of the late starburst population model [Myr]	30, 100, 9000
Mass fraction of the late burst population	0.0, 0.01, 0.1, 0.3, 0.5
Age of the main stellar population in the galaxy [Myr]	500, 1000, 3000, 5000, 10000
Age of the late burst [Myr]	50, 100, 300
Stellar population: `bc03`	
Initial mass function	Chabrier
Metallicity	0.02
Dust attenuation: `dustatt_modified_CF00`	
Av_ISM	0.3, 0.6, 1.0, 1.6, 2.3, 3.0, 3.8, 5.0
Power-law slope of the attenuation in the ISM	−0.7
Power-law slope of the attenuation in the birth clouds	−1.3
Dust emission: `dl2014`	
Mass fraction of PAH	0.47, 1.12, 2.50, 3.90
Minimum radiation field	1.0, 5.0, 10.0, 25.0, 40.0
Power-law slope index $\tilde{\alpha}$ ($dU/dM \propto U^{\tilde{\alpha}}$)	2.0
Fraction illuminated from $U_{\rm min}$ to $U_{\rm max}$	0.1
AGN emission: `fritz2006`	
Ratio of the maximum to minimum radii of the dust torus	60
Optical depth at 9.7 μm	1.0, 6.0
Radial gas density gradient in the torus, β	−0.5
Angular gas density gradient in the torus, γ	4.0
Full opening angle of the dust torus	100.0
Angle between the equatorial axis and line of sight	0.001, 60.100, 89.990
AGN fraction ($f_{\rm AGN}$)	0.0, 0.1, 0.15, 0.2, 0.3, 0.4, 0.45, 0.5, 0.6, 0.7, 0.75, 0.8, 0.9
Radio emission: `radio`	
FIR/radio correlation coefficient $q_{\rm FIR}$	1.5, 1.7, 2.0, 2.15, 2.3, 2.45, 2.58, 2.7, 2.8
Power-law slope α of the synchrotron emission	0.8

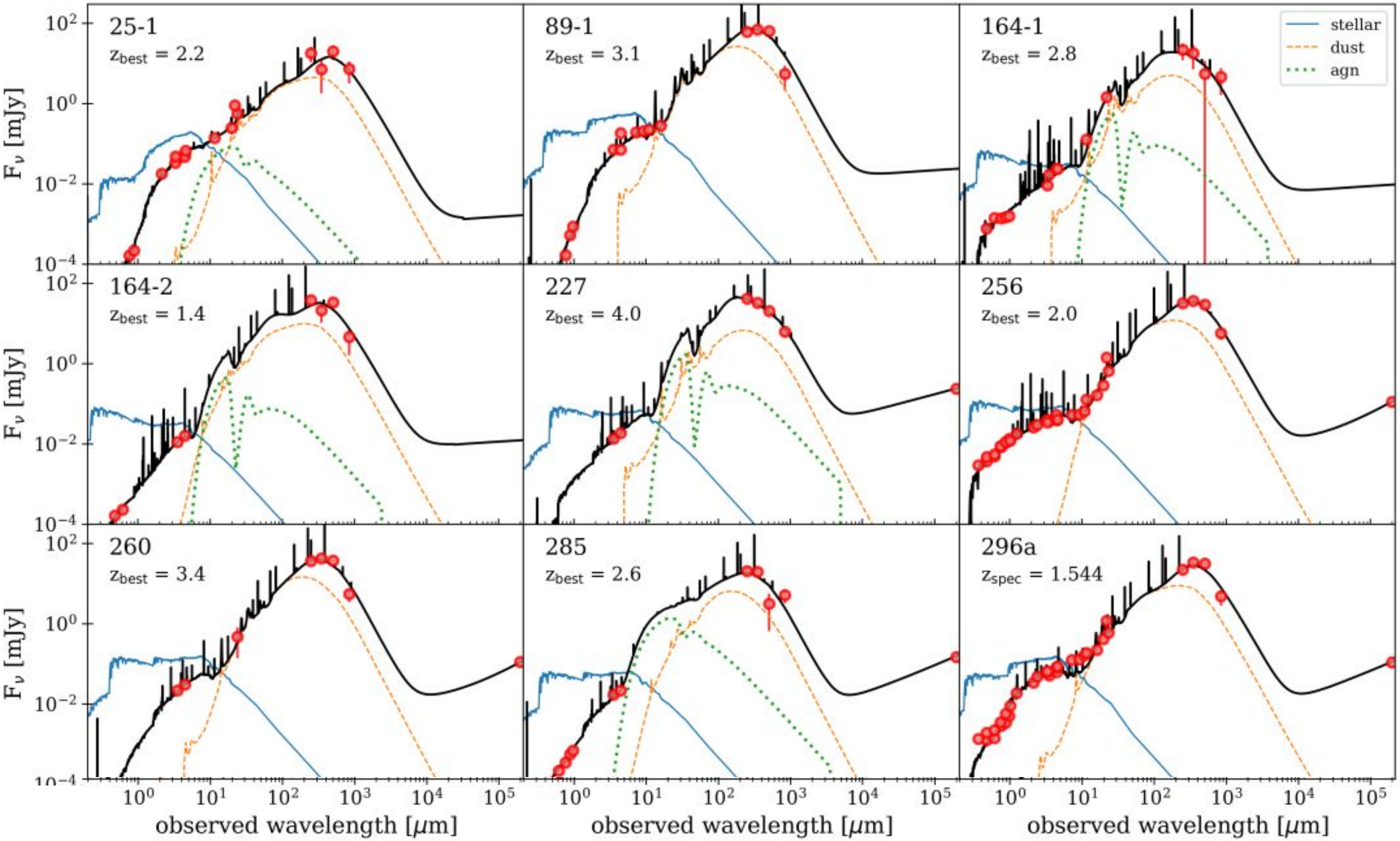

25-1
z_{best} = 2.2
89-1
z_{best} = 3.1
164-1
z_{best} = 2.8
stellar
dust
agn
164-2
z_{best} = 1.4
227
z_{best} = 4.0
256
z_{best} = 2.0
260
z_{best} = 3.4
285
z_{best} = 2.6
296a
z_{spec} = 1.544
F_ν [mJy]
observed wavelength [μm]

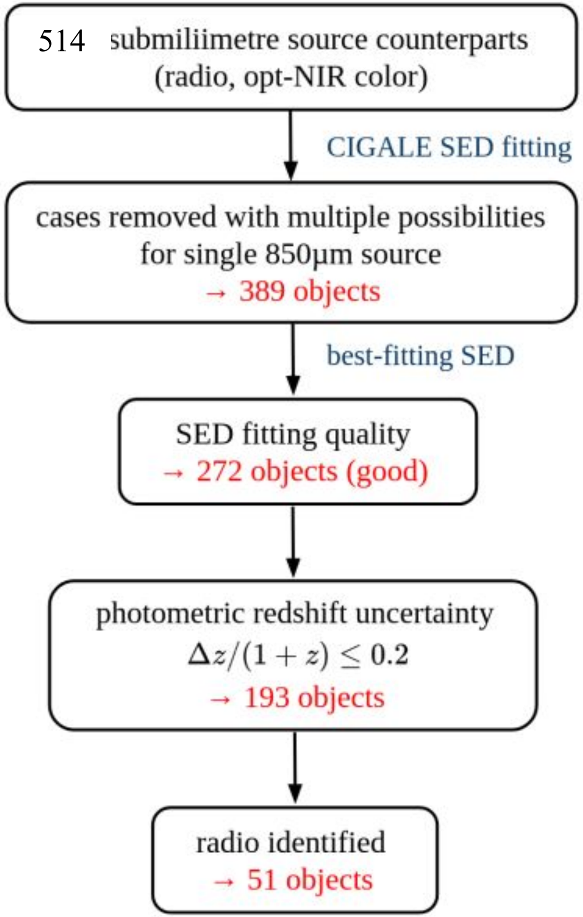

SED fitting results

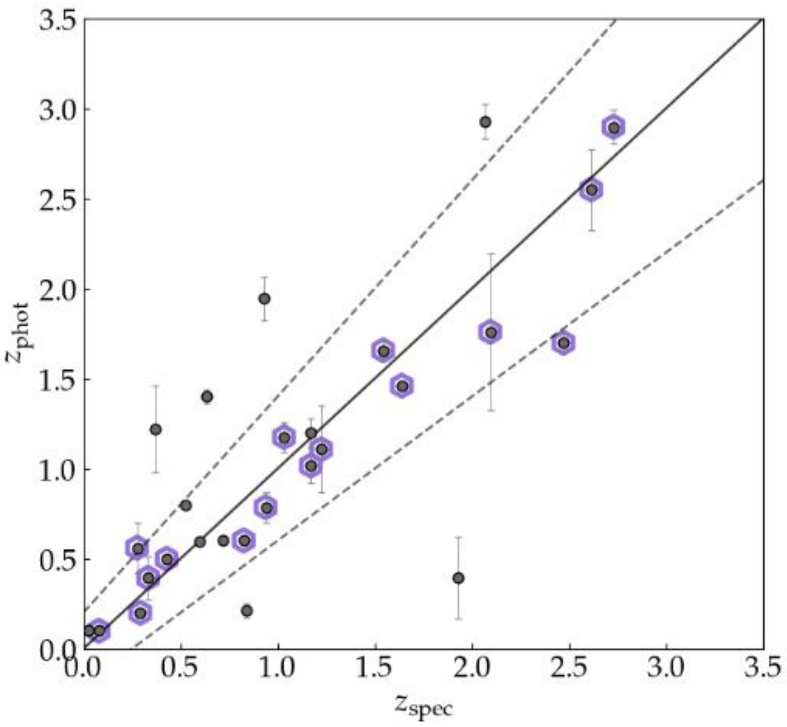

good spectroscopic redshift quality flag

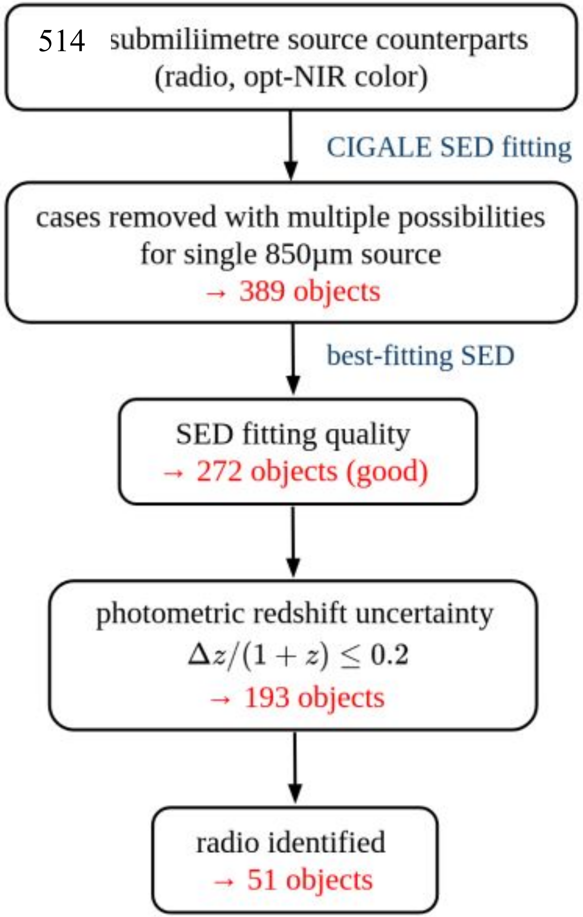
514 submiliimetre source counterparts
(radio, opt-NIR color)
CIGALE SED fitting
cases removed with multiple possibilities
for single 850μm source
→ 389 objects
best-fitting SED
SED fitting quality
→ 272 objects (good)
photometric redshift uncertainty
$\Delta z/(1+z) \leq 0.2$
→ 193 objects
radio identified
→ 51 objects

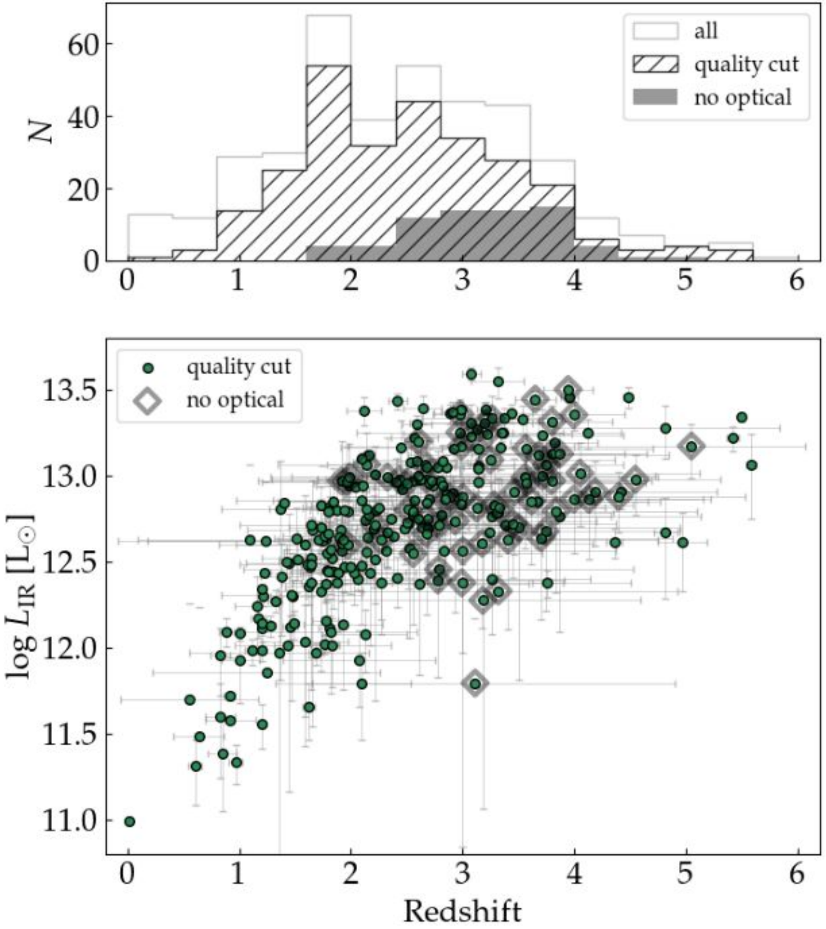
N
all
quality cut
no optical
quality cut
no optical
log $L_{\rm IR}$ [$L_\odot$]
Redshift

SED fitting results

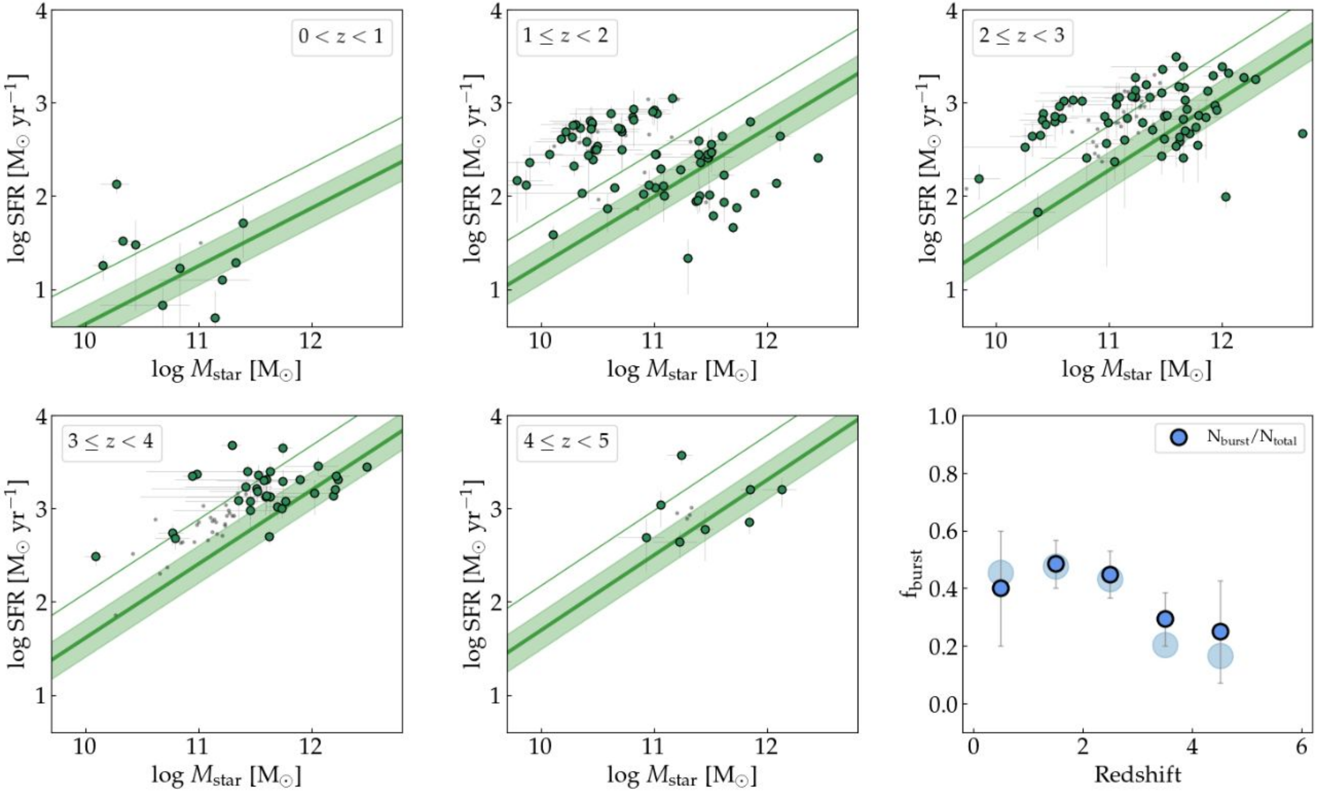

Speagle et al.(2014)
star-forming galaxy main sequence
(**thick**), ×3 SFR (thin)

$f_{burst} = N_{burst}/N_{total}$

~ 40 per cent of SMGs show short timescale for starburst

SED fitting results

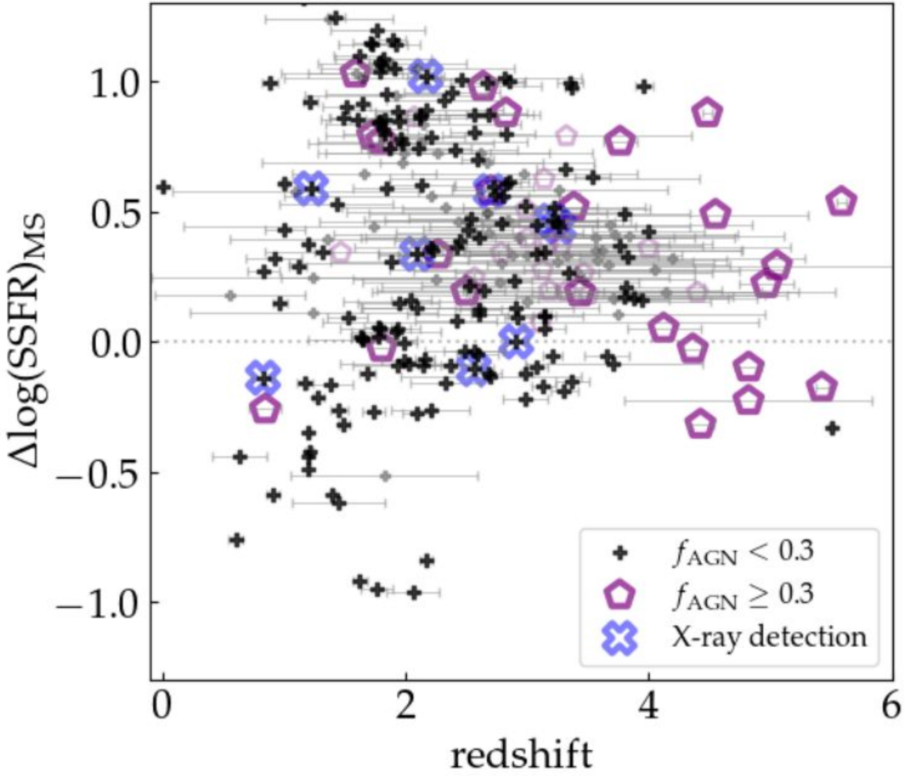

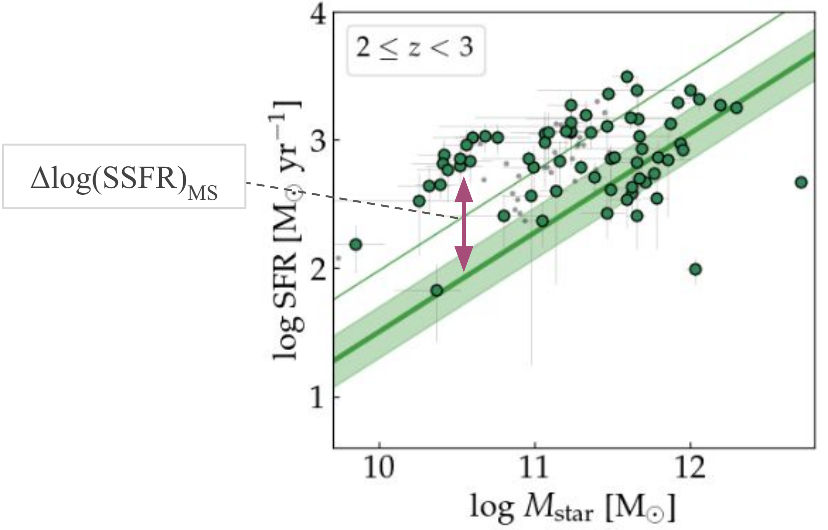

No statistical difference in SSFR between AGN-dominated vs. non AGN-dominated SMGs.

SED fitting results

Barger+2000, submm/radio ratio vs. redshift
(assuming Arp 220 with T_{dust} = 47K)

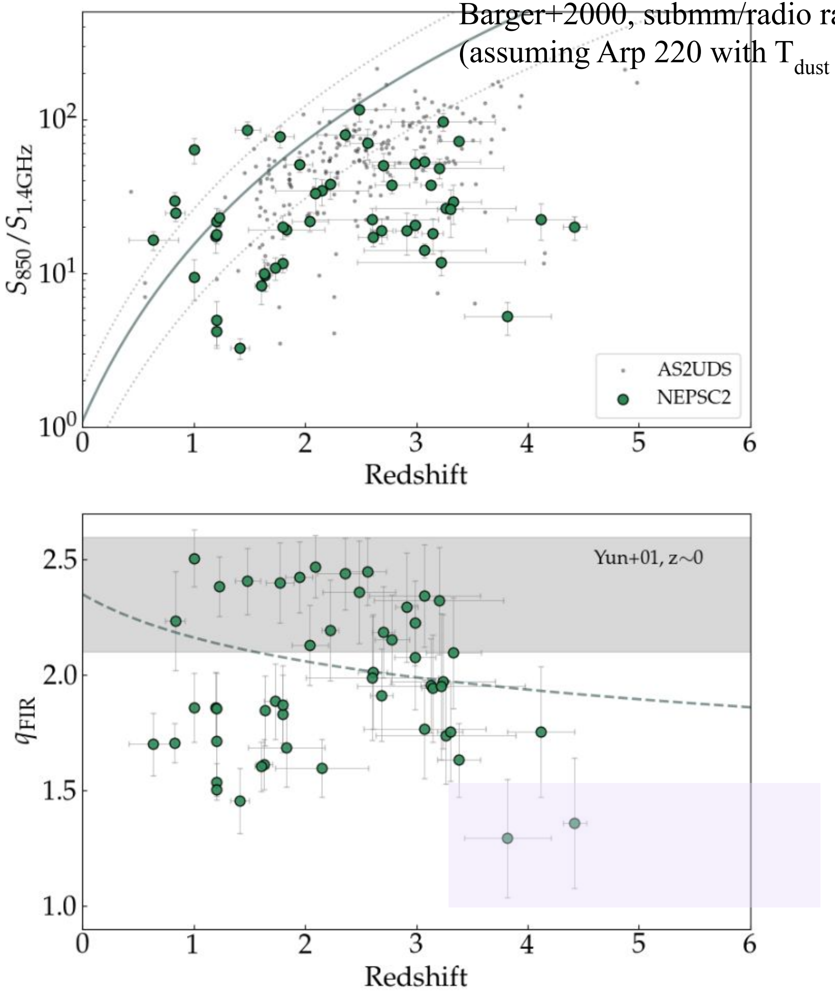

Possible radio-loud AGN candidates at z > 3

Summary

- 647 unique 850μm sources are detected in the NEP field (extending coverage 0.6 → 2deg^2)

- Counterpart identification of SMGs in the 2deg^2 of the NEP field
  - Counterpart(s) were successfully identified for 69% (449/647) of the 850-μm SMGs.
  - The median value of the redshift distribution is <z>=2.5±1.0.

- Star formation, AGN contribution to SMGs
  - Around 40% of SMGs show more than 3 times larger SFR than main sequence galaxies.
  - AGN contributions are relatively high in z>3 SMGs.

850μm maps, source catalogs are publicly available

Counterpart identifications + multi-wavelength photometry + SED fitting results will be publicly available once the paper is accepted.